Journal of Machine Engineering, Vol. 14, No. 4, 2014

both-side drive, synchronous control, cascade regulation,
eigen and locked-motor frequencies, eigenmodes

Vojtech MATYSKA[1*]

BOTH-SIDE DRIVE OF A BALL SCREW FEED AXIS – VERIFICATION OF THE THEORETICAL ASSUMPTIONS

A parallel run of two drives connected in synchronous position control is mainly used in feed axes of gantry machine tools in order to compensate skewing of the gantry. Other reasons for using this concept include increasing rigidity, improving dynamics or achieving thermal symmetry. In most cases these applications use separate position measuring for each drive. Therefore both drives are equivalent in terms of regulation conditions. Due to the mainly used symmetrical design of the axis, the mechanical structure of drives and regulation schema connected to them are also identical. This paper aims to show the results of using two permanent magnet synchronous motors (PMSM) as two drives of the ball screw axis, which is typically and sufficiently controlled with only one drive. The following topics are discussed in this paper: changes in the mechanical structure and its dynamic behavior, effects of this concept on drive regulation and improvements in regulation parameters.

1. INTRODUCTION

The main demands placed on the NC machine tool feed drive axis are high precision positioning and high dynamics. Important prerequisites for achieving these contradictory requirements are stiff and lightweight design of the feed drive axis. These parameters determine the value of the first locked-motor frequency, which limits the gain settings of speed and position cascade controllers. The settings of these gains are also influenced by the type of the drive used and its structure. One of the new concepts is both-side drive with direct encoding of position.

Today, the concept of the both-side drive of the feed axis is not frequently used, except for cases where there are not any other options (such as gantry machine tools or a feed axis with a master-slave drive). Only few companies have presented this or similar concept at well-known exhibitions such as EMO. FANUC developed its “Tandem Control” that allows control over two PMSM in various arrangements. The official documentation says that Tandem Control enables accurately synchronized driving of two motors in the case of one feed axis drive. This original control technology shares control status between two drives. Special interference suppressing algorithm, Tandem Disturbance Elimination Control,

[1] CTU, Faculty of Mechanical Engineering, RCMT, Prague, Czech Republic
[*] E-mail: V.Matyska@rcmt.cvut.cz

cancels interference between the drives and achieves both high gain and stability. Tandem Control can be also applied to a spindle axis. Some possibilities are shown in Fig. 1.

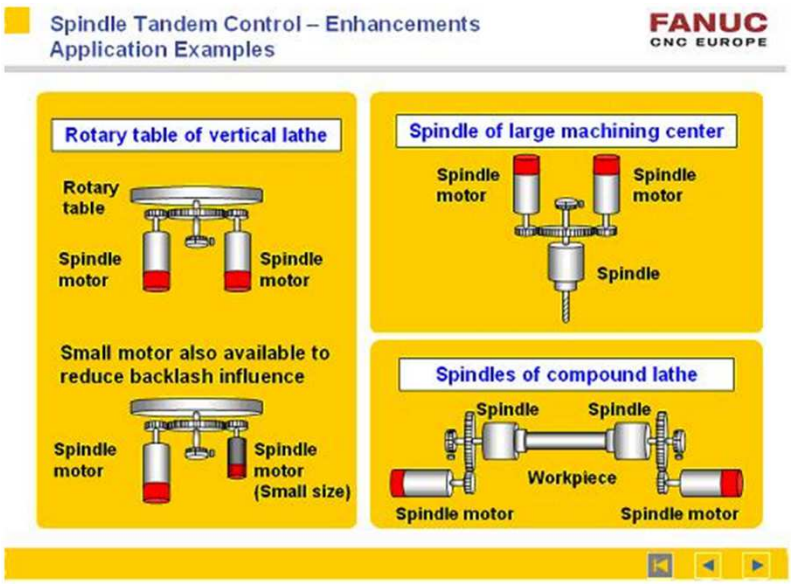

Fig. 1. Examples of Tandem Control [2]

The concept of the both-side drive was also presented by the MCM company on EMO 2009. The i.Tank 1300 machine tool made by this company uses two PMSM with a ball screw of the X axis, i.e. the movable column. Fig. 2 shows the design of the axis and both motors are marked.

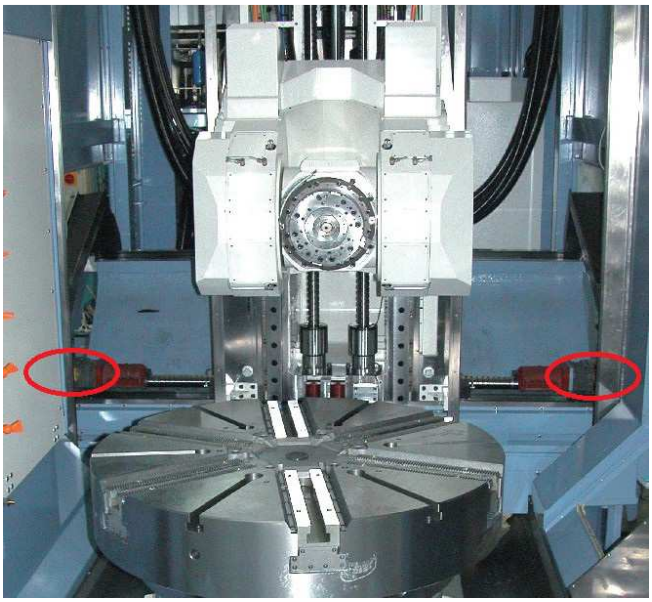

Fig. 2. Axis X of i.Tank 1300 (MCM)

According to MCM description, the both-side drive helps to improve speed, acceleration, precision and rigidity. The machine tool also has symmetrical design, which improves for example thermal behavior.

There is a Japan patent [3] which describes the usage of 2 PMSMs on one ball screw. Primarily, this patent only focuses on one of the results of using the both-side drive, namely reduction in the moment of inertia of motors and screw assembly, which leads to an increase in the maximal acceleration of the feed axis.

Theoretical analysis of the both-side drive concept is in detail provided in [2]. Main parts of this paper are included and summarized in chapter 2 because many results described later can be explained using the conclusions drawn in this analysis. On the other hand, some properties, expected by theory, were not achieved in practical measurement. These differences are also explained.

This paper describes the application of the both-side drive in the design of a test bed with a long ball screw, creating a virtual complex model of the test bed and performing measurements to determine improvements that can be achieved by using this both-side drive concept.

2. THEORY

A commonly used method for the mathematical description of any mechanical structure, including machine tools, is the matrix form of the second Newton's law of motion (modified for constant mass and with expressed forces of rigidity and viscous damping):

$$\boldsymbol{M}\ddot{\boldsymbol{x}}(t)+\boldsymbol{B}\dot{\boldsymbol{x}}(t)+\boldsymbol{K}\boldsymbol{x}(t)=\boldsymbol{f}(t) \tag{1}$$

where:

$\boldsymbol{x}(t)$ is the column vector of actual displacements of n degrees of freedom (DOF) of the described mechanical system,
$\boldsymbol{M}$ is the constant symmetrical matrix ($n\times n$) of mass,
$\boldsymbol{B}$ is the constant symmetrical matrix ($n\times n$) of viscous damping,
$\boldsymbol{K}$ is the constant symmetrical matrix ($n\times n$) of rigidity,
$\boldsymbol{f}(t)$ is the column vector of actual forces (or torques) acting on each of n DOF.

If (1) is transformed with the Laplace transform, $\boldsymbol{x}(s)$ can be expressed as:

$$\boldsymbol{x}(s)=\left(s^2\boldsymbol{M}+s\boldsymbol{B}+\boldsymbol{K}\right)^{-1}\boldsymbol{f}(s) \tag{2}$$

A substitution is commonly performed:

$$\left(s^2\boldsymbol{M}+s\boldsymbol{B}+\boldsymbol{K}\right)^{-1}=\boldsymbol{G}(s) \tag{3}$$

where:

$\boldsymbol{G}(s)$ is the symmetrical matrix ($n\times n$) of transfer functions between inputs (forces) and outputs (displacements) of the system.

Composition of all three matrices in (1) is a separate task. It can be easy for a simple system, such as a few masses connected with springs. In this case computation of $\boldsymbol{G}(s)$

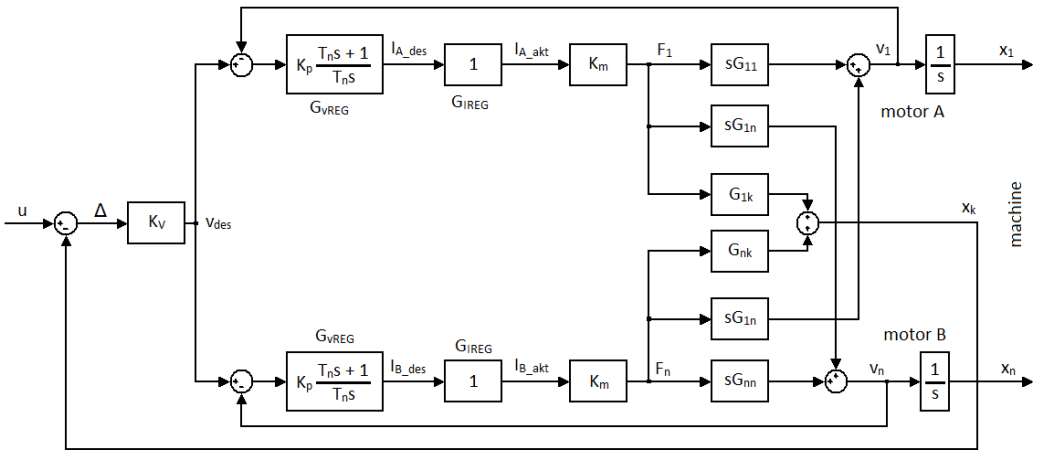

Fig. 3. Block diagram of both-side drive

should not be a problem. Simple examples in [2] are prepared in this manner. However, it can be very difficult, or even impossible, for systems with continuously spread properties such as real machines. In such cases these systems are discretized by the FE method. A lot of FEM software is available today, although it commonly does not export matrices $\boldsymbol{M}$, $\boldsymbol{B}$ and $\boldsymbol{\kappa}$ and uses different methods to evaluate desired matrix $\boldsymbol{G}(s)$.

Matrix $\boldsymbol{G}(s)$ is used to evaluate influences of torque of motors on displacement of each motor and point of position measurement. Let us assume that in the system of n degrees of freedom, x_1 coordinate is assigned to rotation of the first motor A, x_n coordinate is assigned to rotation of the second motor B of the same axis and x_k coordinate is assigned to direct position encoding. In most cases, when 2 PMSMs are used, these motors are the same and the mechanical structure of the drive is symmetrical. So let us assume that control loops of both motors are also identical. Then let us assume that current control loops (G_{IREG}) are perfect, so actual current I_{x_act} equals desired current I_{x_des} for all frequencies (index x is used to denote the particular motor). Based on these assumptions a block diagram of mechanical system regulation can be composed, using the both-side drive concept and cascade regulation (see Fig. 3). Thanks to direct position encoding only one position control loop is needed and desired speed v_{des} is shared by both speed control loops.

Setting of speed control loop is crucial for the resulting properties of the machine tool axis [1], so diagram in Fig. 3 is used to evaluate command frequency response of the speed control of both motors:

$$W_A(s)=\frac{v_1(s)}{v_{des}(s)}=\frac{sG_{vREG}\left(G_{11}+G_{1n}\right)+s^2G_{vREG}^2\left(G_{11}G_{nn}-G_{1n}^2\right)}{1+sG_{vREG}\left(G_{11}+G_{nn}\right)+s^2G_{vREG}^2\left(G_{11}G_{nn}-G_{1n}^2\right)} \tag{4}$$

$$W_B(s)=\frac{v_n(s)}{v_{des}(s)}=\frac{sG_{vREG}\left(G_{nn}+G_{1n}\right)+s^2G_{vREG}^2\left(G_{11}G_{nn}-G_{1n}^2\right)}{1+sG_{vREG}\left(G_{11}+G_{nn}\right)+s^2G_{vREG}^2\left(G_{11}G_{nn}-G_{1n}^2\right)} \tag{5}$$

As can be seen, the transfer function of speed controller G_{vREG} cannot be separated from the numerator of both responses, so zeros (equivalent to locked-motor frequencies) of these responses are influenced by speed control and its settings. As will be shown later, speed control in the both-side drive can significantly affect some locked-motor frequencies of the mechanical system. This is impossible with standard speed control with only one motor.

Special attention in [2] is paid to a distinct modification of the mechanical system, specifically to completely symmetrical systems. Machine tools are frequently designed symmetrical, so the attention is legitimate. Matrices $\boldsymbol{M}$, $\boldsymbol{B}$, $\boldsymbol{K}$ and even transfer function matrix $\boldsymbol{G}(s)$ of these systems are symmetrical along the main skew diagonal, so transfer functions G_{11} and G_{nn} are identical. This equality allows simplification of command frequency responses (4) and (5):

$$W_A(s)=W_B(s)=\frac{sG_{vREG}\left(G_{11}+G_{1n}\right)}{1+sG_{vREG}\left(G_{11}+G_{1n}\right)} \tag{6}$$

Equation (6) implies that zeros of response originating in mechanical system are not now influenced by the speed control loop. However, as shown in [2], more significant changes appear in transfer function $\left(G_{11}+G_{1n}\right)$. Denominators of any transfer function G_{ij} of the system with n degrees of freedom are the same polynomial of Laplace operator s, and has degree $2n$. This also applies to the sum $\left(G_{11}+G_{1n}\right)$ of all non-symmetrical systems. But when the system is symmetrical, the degree of $\left(G_{11}+G_{1n}\right)$ is lowered, so the system appears as though it has less eigen- and locked-motor frequencies, when controlled with the both-side drive.

These omitted eigenfrequencies correspond to eigenmodes that are anti-symmetric, i.e. motors oscillate with the same amplitude but in the opposite direction (phase shift between the two motors is exactly 180°). This effect is not influenced by the speed control loop either. It always occurs in the symmetrical system.

But even symmetrical machines do not have to be symmetrical in terms of dynamics. Any displacement of a linearly movable part of the axis out of the middle position causes that the resulting system is not entirely symmetrical. And the mentioned anti-symmetrical eigenmodes became only nearly anti-symmetrical. It was assumed that similar, but not completely ideal, influence of the both-side drive take effect, so these nearly antisymmetrical modes would be almost completely omitted i.e. considerably damped. It will be shown in this paper that this assumption was not generally correct and could be made only under certain circumstances.

All mentioned theoretical results were tested on a simple 4-mass test-bed and were confirmed by performed measurements. The measurements and conclusions based on them are also included in [2].

3. TEST-BED DESIGN AND AN FE MODEL

To support theoretical results mentioned in [2] and subsequently in chapter 2, a test-bed (called STD-3) was designed and built. This test-bed was planned to prove that the both-side drive can be applied to a ball screw axis with all its effects. It was also decided to design STD-3 similar to the real axis of a machine tool, so the proof would be convincing STD-3 stands on a modified old grinding machine bed. The effect of the usage of 2 PMSMs could be demonstrated more easily on a long ball screw, so the length of the screw was designed up to ca 2,000mm with respect to critical rotation speed and buckling stress. Beside the length, the chosen diameter of 32mm makes the screw very flexible. Still, the flexibility of the couplings used is more significant. The screw has an axial-radial bearing on one end and a radial bearing on the other, both housed in motor holders. Baumüller motors of the same type are also mounted to them and connected to the ball screw by a pair of steel bellows couplings. The design of the sliding table, connected to the ball screw nut, allows various structural modifications, so STD-3 can simulate an axis with a simple and light table (weight 54kg), with a heavy table (for example a rotary table of higher design or a simple table with a loaded workpiece – weight 220kg) or an axis with a sliding column (total weight 275kg).

All these variants can be driven in two modes, as a classical ball screw axis with only one motor or as an axis with the both-side drive. As both modes should be interchangeable, torque of a single motor in the classical mode should be equal to the total torque of both motors in the both-side drive. This is ensured by torque margin set to one half of the maximum torque when operating in the both-side drive mode because only one type of PMSM is used. Stronger motors used in real machine tools also have greater moment of inertia, which is compensated in STD-3 by an additional weight connected to the motor shaft when operated in the classical mode. Therefore real conditions are simulated in the best possible manner in both modes.

Based on the described design, test-bed STD-3 was assembled (see Fig. 4) and also an FE model was created. Details of motor A with and without the additional weight are also shown in Fig. 4.

After the FE model was made, it had to be verified for several reasons. Some parameters, like Young's modulus of cast iron, which machine bed is made from, were unknown. In the case of cast iron only a rough estimate of the modulus $(0.8 \div 1.25)\cdot 10^5$MPa was available. After some measurements and test computations, the final value $1.1\cdot 10^5$MPa was determined. Some other parameter values could be found in catalogues, but a comparison of measurements and model results reveals that these values are inaccurate. For example, torsion stiffness of the coupling is stated as 9,000Nm·rad^{-1} but the measured value subsequently used in the FE model is only 5,000Nm·rad^{-1}. Another reason why verification is required is that the FE model is simplified and these simplifications have to be proved as negligible. So a series of basic measurements was performed and the FE model was corrected so that it would closely match the measured results. A model of the mechanical system (i.e. transfer function matrix $\boldsymbol{G}(s)$) was prepared based on this corrected FE model.

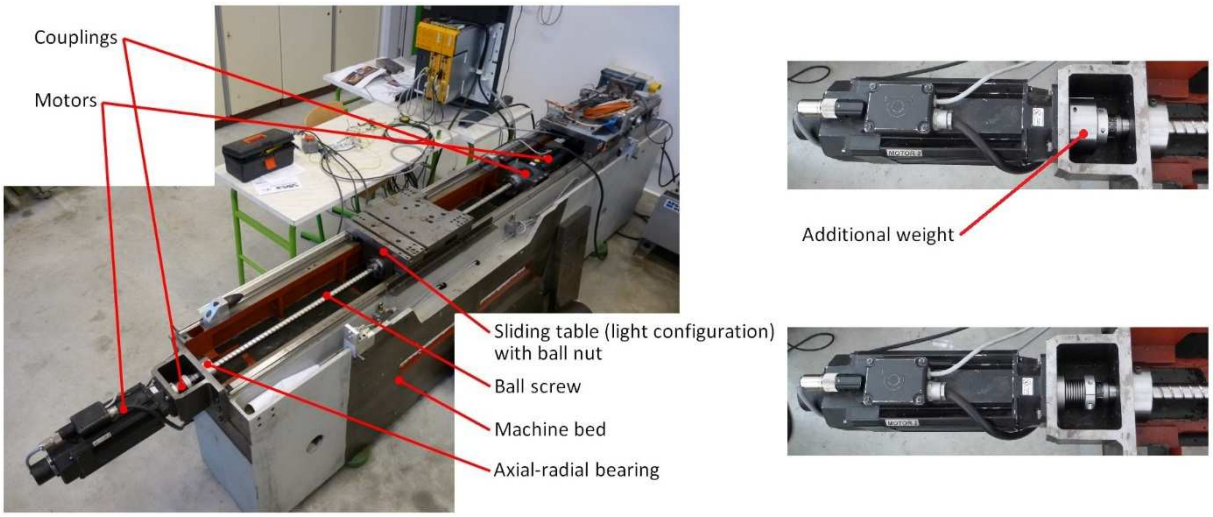

Fig. 4. Actual design of STD-3

STD-3 is controlled with two identical Baumüller servo controllers connected to motors and configured in such a way that speed control loops are closed in their control system (Fig. 5). Signals of desired speed v_{des} are transferred to the servo controllers via their analogue inputs. The signal of v_{des} is generated in the controlling computer by MATLAB software and is divided for each servo controller and sent on analogue outputs of measuring PCI card using MATLAB Real Time Toolbox. Outputs of the card are connected to the inputs of the servo controllers. This connection between the controlling computer and servo controllers has many advantages, such as complete control over drive type (easy switching between classical and both-side drive), possibility of any shaping of control signals of speed and position etc.

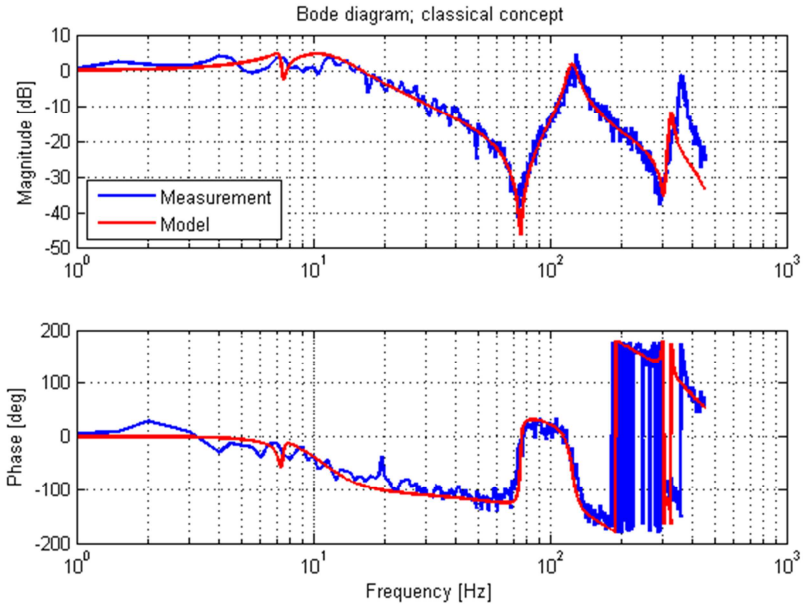

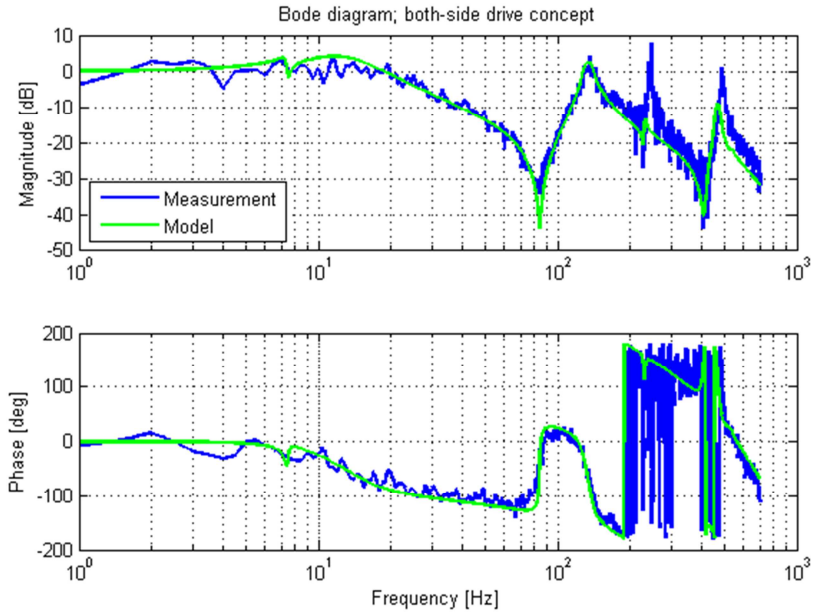

Fig. 5. Speed control loop transfer function of STD-3 in both concepts

But it also has one disadvantage: sampling time of analogue inputs of servo controllers is considerably high, which worsens the quality of speed control. But it does not pose any problem because the sampling time and its influence is the same for all measurements, so all measurements will be comparable. It just has to be taken into account in the drive regulation model connected to the model of the mechanical system represented by matrix $\boldsymbol{G}(s)$. The drive regulation model also takes into account the bandwidth of the current control loop.

4. CLASSICAL AND BOTH-SIDE DRIVE COMPARISON

The FE model of STD-3 was made and verified because of three main reasons. The first was to ensure that the both-side drive can be simulated even on a more complicated model. The second was to gain more information about the mechanical system. When measuring the transfer function of the speed control loop, we obtain only values of locked-motor frequencies. When the model is verified, FEM software can show eigenfrequencies and corresponding eigenmodes. This helps us to understand which part of the test-bed has a major influence on which eigenmode. And it also enables us to predict, which eigenmode will be damped by the both-side drive. And the third main reason for creating the FE model was visual. Measured transfer functions are always at least slightly noised. When the models for both classical and both-side drive are created, their transfer functions are clear and easily comparable to each other.

The next figures show measured and modelled transfer functions of the speed control loop of STD-3 with a heavy sliding table in the middle of the feed axis driven with only one motor (Fig. 5 on the left), STD-3 driven with two motors in the both-side drive (Fig. 5 on the right) and a comparison of models of both concepts (Fig. 6).

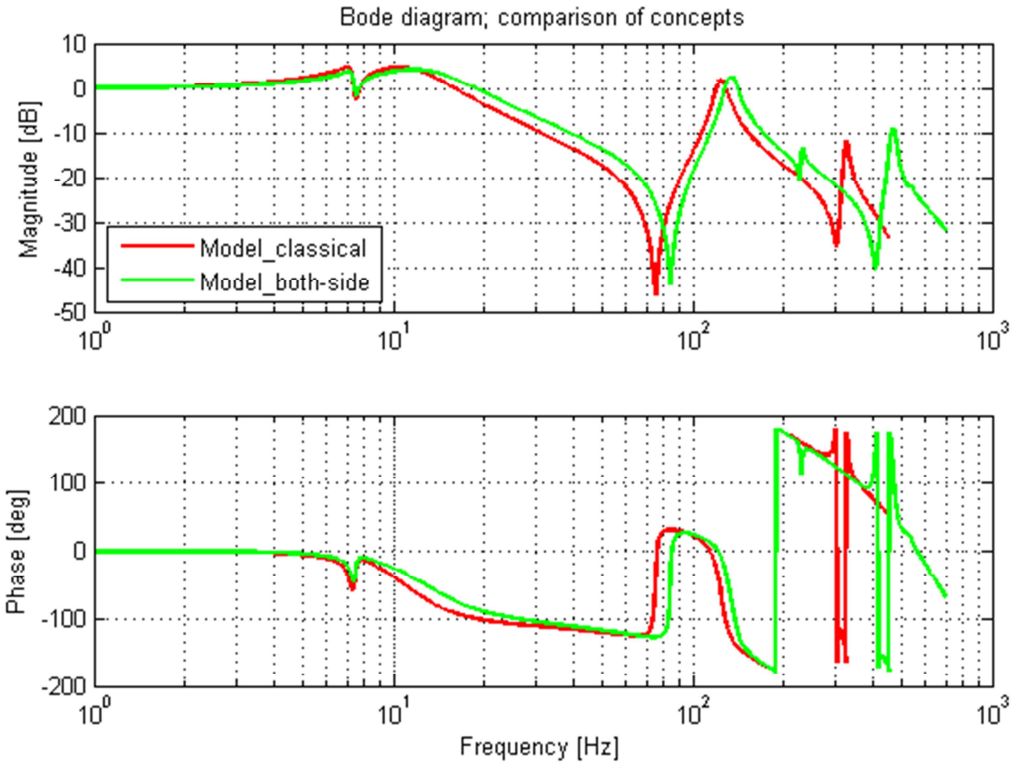

Fig. 6. Comparison of concepts

Measurements in all figures are drawn in blue, the model of the classical concept in red and of the both-side drive in green. As can be seen in Fig. 5, measurements and models are quite similar, only minor differences (under 10% in frequency) are found. Only one major difference in magnitude appears at a frequency of 240Hz and it will be discussed later.

The comparison of both concepts displayed in Fig. 6 shows some effects of the both-side drive. The first locked-motor frequency at 7Hz is not altered because it is connected to rocking of whole STD-3 on elastic mounting to floor. Slight frequency shift of the second locked-motor frequency around 80Hz (and connected eigenfrequency around 130Hz) is caused by differently distributed mass in the system. Total reduced mass of the system is constant because the additional weight used in the classical drive (to simulate heavier motor) has moment of inertia equal to the second motor used in the both-side drive. An eigenfrequency of the both-side drive of 240Hz is the one that corresponds to anti-symmetric eigenmode. In the classical drive it has no equivalent because it appears when the second motor is added. According to the assumption made in chapter 2, it should be damped and not visible in this graph. Why it is not so will be discussed later. Great frequency shift of the next eigenfrequency (325Hz to 466Hz) is caused by using smaller (and lighter) motor. Eigenmode corresponding to this frequency is influenced mainly by the moment of inertia of the motor near the axial bearing and coupling connected to it and by the rigidity of the ball screw nut. And this motor has in this both-side drive one half moment of inertia of the motor used for the classical drive (additional weight is removed). In the real

machine tool the moment of inertia of the motors used would be even smaller, so the resulting properties would be better.

These results were obtained after tuning constants of the speed controller. For this tuning, a test response to the desired speed step was used and the resulting setting was made so that these responses were qualitatively alike (so the speed control loops were comparable). Also the position controllers were tuned using test response to desired position ramp. Table 1 shows all constants for both concepts.

Table 1. Regulation parameters of STD-3 with heavy table

Parameter		Classical drive	Both-side drive
Speed control loop	K_p	$0.215 A \cdot s \cdot rad^{-1}$	$0.143 A \cdot s \cdot rad^{-1}$
	T_n	$0.0125 s$	$0.0125 s$
Position control loop	K_V	$20 s^{-1}$	$30 s^{-1}$

As can be seen, in the both-side drive the proportional gain had to be lowered. It was due to a high measured peak of 240 Hz that limited the bandwidth of the speed control. However, the speed control of the both-side drive was not worse than the speed control of the classical drive, because due to the use of the two motors, effectively only half of the system mass accrued to each of them. The speed control was even slightly better (see Fig. 6). And the proportional gain of the position control also increased. This caused a decrease in the position control deviation (following error) to two thirds compared to the classical drive for the same desired speed.

4.1. ANTI-SYMMETRICAL EIGENMODE AT 240HZ

In this subchapter two issues will be discussed. The first one is why the measured peak at 240Hz is considerably higher than the modelled one. And the second is why these peaks are visible in both transfer functions despite the assumption made in chapter 2.

Let us start with a description based on the FE model of this eigenmode first. Its eigenfrequency is 215Hz (the shift to 240Hz is caused by interaction with the speed controller). The eigenmode could be considered as entirely rotational (all translational movements of all model parts are very small and could be neglected). As can be seen in Fig. 7, which shows dynamic compliance of the mechanical model, this eigenmode (highlighted in red) is very significant. By analysing this eigenmode, it was found out that despite all the efforts this eigenmode is not entirely anti-symmetrical (difference in amplitudes is only 1.7%). The reasons for that are probably the following: the table is not exactly in the middle, only one bearing is axial-radial etc., so the model is not perfectly symmetrical.

Although the deviation from ideal anti-symmetry is small, it still leads to cancelling the effect of lowering degree of the $(G_{11}+G_{1n})$ transfer function, which was mentioned in chapter 2. Therefore the eigenmode is visible in the transfer functions of the speed control loop. However, it is damped by the regulation, though not entirely.

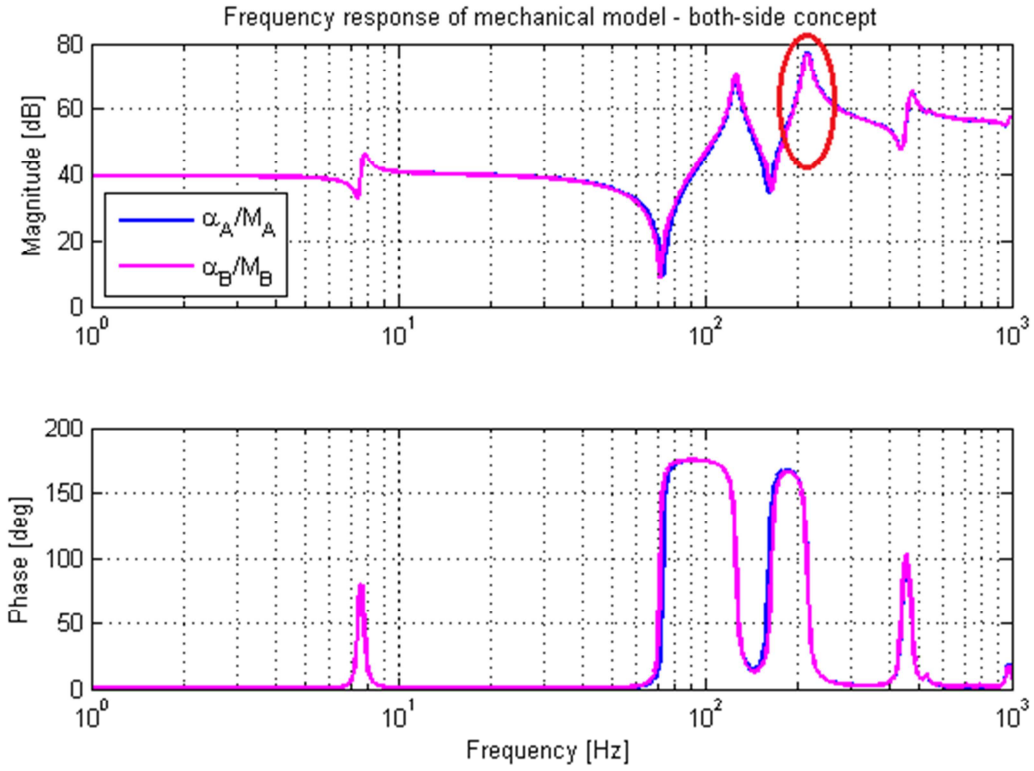

Fig. 7. Dynamic compliance of the mechanical model

The influence of regulation settings is demonstrated on simulation models and shown in Fig. 8. Regulation 1, which has the same settings as the one used in measurement, has a damping effect on this eigenmode. The bandwidth of Regulation 2 is expanded, which is achieved by increasing of the current control loop bandwidth, eliminating of the time delay in the speed control and changing regulation constants to $0.716\text{A}\cdot\text{s}\cdot\text{rad}^{-1}$ for the proportional gain and $2.5\cdot10^{-3}$ s for the integration time constant. And it is clearly visible that better speed control ideally damped this anti-symmetrical eigenmode due to the interaction between mechanics and regulation described in chapter 2. On the other hand, when the regulation constants are changed in the opposite manner ($0.107\text{A}\cdot\text{s}\cdot\text{rad}^{-1}$ and $12.5\cdot10^{-3}$ s – Regulation 3), the eigenmode is not damped at all.

In the measured transfer function of speed control loop this eigenmode has an even more distinctive peak. It is because STD-3 has more differences from ideally symmetrical structure. Couplings have probably different torsion stiffness (because of production variations and different assembly) which cannot be determined. Moreover, servo controllers

are not connected, so they can sample analogue input signal of desired speed in different time (though on the same sampling frequency), which brings another, this time electrical, asymmetry. And the more differences there are from ideal symmetry, the lower the effect of the speed control is and the greater the decrease in damping of the anti-symmetrical eigenmode is.

In the measured transfer function of speed control loop this eigenmode has an even more distinctive peak. It is because STD-3 has more differences from ideally symmetrical structure. Couplings have probably different torsion stiffness (because of production variations and different assembly) which cannot be determined.

Moreover, servo controllers are not connected, so they can sample analogue input signal of desired speed in different time (though on the same sampling frequency), which brings another, this time electrical, asymmetry. And the more differences there are from ideal symmetry, the lower the effect of the speed control is and the greater the decrease in damping of the anti-symmetrical eigenmode is.

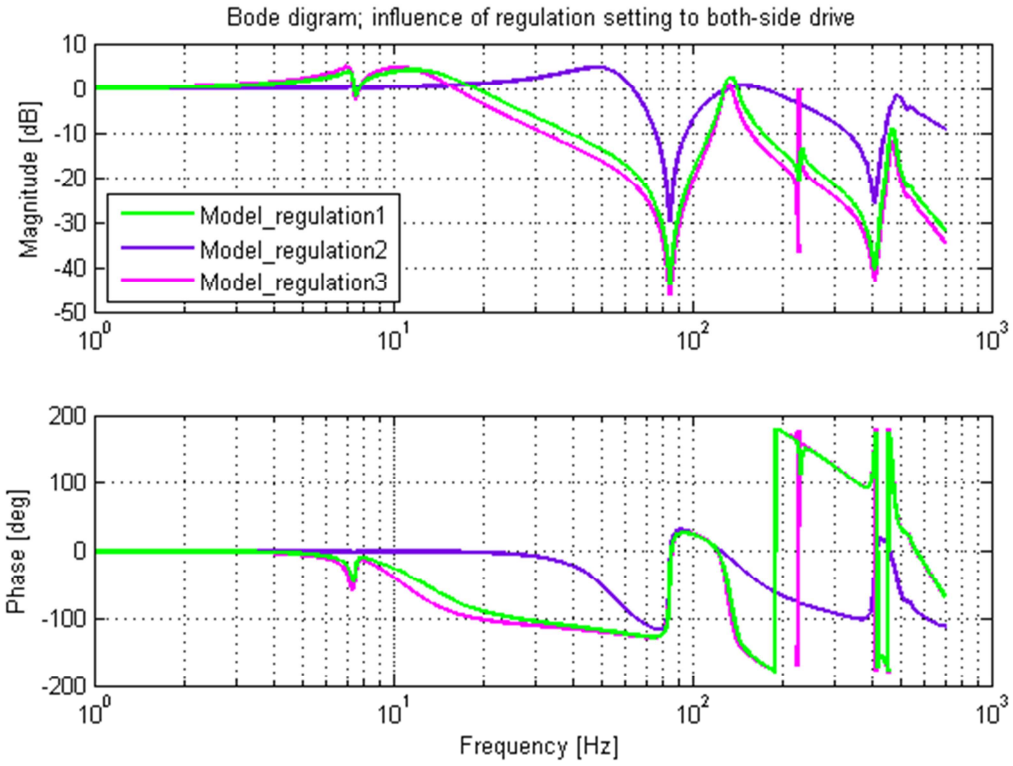

Fig. 8. Influence of speed control loop bandwidth

Although the 4-mass system, which all theoretical results were tested on, is also asymmetrical, significant damping of one particular eigenmode (and corresponding locked-motor frequency) in the measured transfer function of the speed control loop can be seen [2]. The reason for this is that in all cases described in [2] the examined eigenmode was inside the bandwidth of the speed control loop, where the speed control could adjust it, i.e. damp it, similarly to the case of Model_regulation 2 in Fig. 8.

5. SUMMARY

Damping effects on eigenmodes that are caused by the both-side drive can be divided into two categories. Anti-symmetrical eigenmodes of the ideally symmetrical mechanical structure are completely suppressed independently on the speed control. This is the entirely mechanical influence of the both-side drive. But even very small deviation from symmetry cancels this effect. And most systems are not symmetrical, either due to machine design or due to the position of sliding parts. The almost anti-symmetrical eigenmodes of the asymmetrical mechanical structure can be damped too. It only depends on the actual eigenmode and its eigenfrequency in relation with the bandwidth of the speed controller. The less anti-symmetrical the eigenmode is, the higher the bandwidth must be compared to the eigenfrequency. And when the bandwidth is sufficient, the eigenmode is damped by the speed control of the both-side drive.

The both-side drive has a number of advantages. Feed axis has mostly better dynamical behaviour (by lowering mass of some components) and potential to damp eigenmode that appears with adding the second motor. The total reduced moment of inertia of movable parts can be lower due to using smaller motors while keeping all other parameters of the axis like max speed and max force the same or better. And this can save energy in the case of axes that often accelerate and brake. And most importantly, position control proportional gain can be significantly increased (so the position control will be more accurate).

The only disadvantage is the higher cost of this concept. New parts have a minor influence on the total price because the need to purchase an additional motor and servo controller is balanced by the lower price of the weaker equipment. The biggest increase in price is caused by enabling control of more axes in synchronous mode.

REFERENCES

[1] GROß H., HAMANN J., WIEGÄRTNER G., 2001, *Electrical feed drives in automation*, Munich: Publics MCD Werbeagentur GmbH, ISBN 3-89578-148-7.

[2] SOUČEK P., NOVOTNÝ L., RYBÁŘ P., 2009, *Research of drive regulation of NC machine tool feed axes – Part A*, Report V-09-061, Czech Technical University in Prague, Faculty of Mechanical Engineering, Research Center of Manufacturing Technology, (in Czech).

[3] KITAMURA K., YAMADA S., 2009, *Drive unit for NC machine tool*, Patent JP2001259953 (A), Japan, KITAMURA MACHINERY CO LTD.